



THE IMPACT OF NON-STRUCTURAL COMPONENTS ON FRAGILITY CURVES OF SINGLE-STOREY INDUSTRIAL PRECAST BUILDINGS

A. Babič⁽¹⁾, M. Dolšek⁽²⁾

⁽¹⁾ PhD Student, University of Ljubljana, Faculty of Civil and Geodetic Engineering, Anze.Babic@fgg.uni-lj.si

⁽²⁾ Professor, University of Ljubljana, Faculty of Civil and Geodetic Engineering, Matjaz.Dolsek@fgg.uni-lj.si

Abstract

Fragility curves for six classes of precast buildings are presented. Only the type of non-structural components was varied in order to define different variants of investigated building classes. Precast buildings without non-structural components represented a base case of investigation. In addition, one building class with vertical panels, one with masonry infills and three building classes with horizontal panels were defined, each with a different type of panel-to-structure connections. Each building class was represented by a sample of 100 buildings. For each building a simplified three dimensional numerical model was built, in order to perform a large number of non-linear dynamic analyses, but still capable to account for phenomena such as panel-to-structure interaction, infill-to-structure interaction, sliding of the unrestrained elements and accounting for the non-structural components only until the point of their dislocation. Based on the simulations, fragility curves for three non-structural damage states and two structural damage states were developed. It can be observed that the type of the non-structural components had a detrimental impact on all levels of damage, including structural collapse. In addition, the effect of non-structural components is illustrated using an example of a non-linear dynamic analysis. It is shown that the mass of non-structural components had in most investigated cases detrimental effect on damage, whereas the effect of increased stiffness proved to be more unfavourable if the non-structural components are attached to the structure below the beam-to-column connection rather than above it.

Keywords: fragility analysis; precast buildings; friction connection; non-structural components; nonlinear dynamic analysis

1. Introduction

Single-storey RC precast buildings are among the most common types of industrial buildings in southern and central Europe. Their structures consist of cantilever columns connected at the top by a roof, which is essentially an assembly of precast components. For their façades, horizontal and vertical precast panels and masonry infill walls are most commonly used. These components are considered to be non-structural.

Vulnerability of these type of buildings was revealed several times, most recently during the L'Aquila (2009) and Emilia-Romagna (2012) earthquakes, when many precast buildings, which had been built in the last decades, partly or totally collapsed (Fig. 1). Studies, which have been performed after these events [1-3], highlighted extensive rotations of the columns and insufficient shear capacity of the beam-to-column connections as the most frequent sources of damage. According to these studies, the former occurred due to large flexibility of the structures, whereas the latter resulted from insufficient design of the connections, which in many cases relied only on friction between the column and the beam.

Damage to horizontal and vertical panels and masonry infills has been discussed by several researchers [1-5]. The poor performance of the panels was contributed by the insufficiently designed fastenings, i.e. steel devices, which are provided at the top of the panels in order to prevent them from overturning. More specifically, they were found to be inadequate to withstand the relative displacements between the panels and the structure, leading to the in-plane failure of the panels [1-3]. Moreover, out-of-plane failures of fastenings due to inertial forces perpendicular to the plane of the panels were also reported [3]. In the case of masonry infills, the most frequently observed damage was associated with the infills simply overturning [4, 5], which was attributed to the poor connection with the adjacent beams. In many cases there was no connection at all due to a continuous window at the top of the infill. The Emilia earthquake also revealed that the impact of panels and infills on the overall performance of structures had often been underestimated in the design. Recent studies have confirmed

this observation. According to Bournas et al. [3] only the mass of the panels was considered in the current Italian design practice, whereas the increase in structural stiffness was overlooked, which led to unrealistically high periods and consequently to underestimated design seismic forces. Colombo et al. [6] showed that consideration of the panels is essential if one wants to properly assess the seismic response of precast structures. Ercolino et al. [7] observed reductions in the first vibration period of up to 80 % when the panels were taken into account. Belleri et al. [8] found that configuration of panels affected the vulnerability assessment and retrofit strategies.



Fig. 1 – a) Dislocation of precast vertical panels, and b) collapse of a precast RC building due to the 2012 earthquakes in the Emilia Romagna region.

Although seismic fragility analysis is a well-established method of vulnerability assessment of various classes of buildings, the number of studies which have addressed the seismic fragility of single-storey precast buildings is quite limited. Senel and Kayhan [9] investigated the fragility of typical Turkish precast buildings, whereas Casotto et al. [10] calculated fragility functions for different classes of Italian precast buildings. In these studies, the effect of non-structural components was not taken into account. Korkmaz and Karahan [11] determined fragility functions for precast buildings in Turkey considering the presence of masonry infills. However, only in-plane failure of the infills was taken into account. Babič and Dolšek [12] developed fragility functions of twelve classes of precast building, which contained bare-frame buildings as well as buildings with vertical panels, buildings with horizontal precast panels and building with masonry infills.

In this paper, six building classes, which were investigated by Babič and Dolšek [12], are addressed with an emphasis to provide an insight of the effect the non-structural components on the fragility curves. Firstly, the investigated building classes and their basic characteristics are presented. This is followed by the description of the corresponding numerical models. Then the methodology of development of fragility curves, which was originally proposed in [10] and modified in [12], is briefly described. The results of the fragility analysis are then presented. Firstly, by comparing the parameters of fragility curves of six building classes and for five damage states, and secondly, by an illustrative example of a non-linear dynamic analysis, which explains the phenomena caused by the presence of the non-structural components.

2. Investigated building classes

Six classes of single-storey precast buildings were investigated (Table 1). All the building classes had the same load-bearing structure, but contained different type of non-structural components. Buildings without non-structural components, buildings with vertical panels and buildings with masonry infills were each represented by one building class, whereas three building classes of buildings with horizontal panels were defined, each with a different type of fastenings, which are essentially steel devices provided at the top of the panels, in order to prevent them from overturning. Basic information about the investigated building classes is given in the following, while more details are given in previous studies [10, 12].

Table 1 – Definition of considered classes of precast buildings

Building class	Non-structural components	Fastening
1	None	/
2	Vertical panels	A
3	Horizontal panels	A
4	Horizontal panels	B
5	Horizontal panels	C
6	Masonry infills	None

The load-bearing structures consist of cantilever columns, which support long saddle beams covered by roof elements (Fig. 2a). The beam-to-column connections contain no mechanical elements and rely only on friction. The basic geometrical parameters are presented in Table 2. The cross-sectional heights (equal to 50 cm) and longitudinal reinforcement ratios (with the mean and the standard deviation equal to 1.13 % and 0.22, respectively) of the columns were determined on the basis of the building code which was in force at the time of the design [10] and was associated with a design lateral load equal to two percent of the buildings' self-weight. The values of the mechanical characteristics of the materials prescribed in the design are given in Table 3. A low transverse reinforcement ratio was assumed in all parts of columns, resulting in a confinement coefficient equal to 1.00. Furthermore, the differences between the actual material properties used in the modelling (Section 3) and the design values indicated in the codes were accounted for by making use of overstrength factors as described in [10].

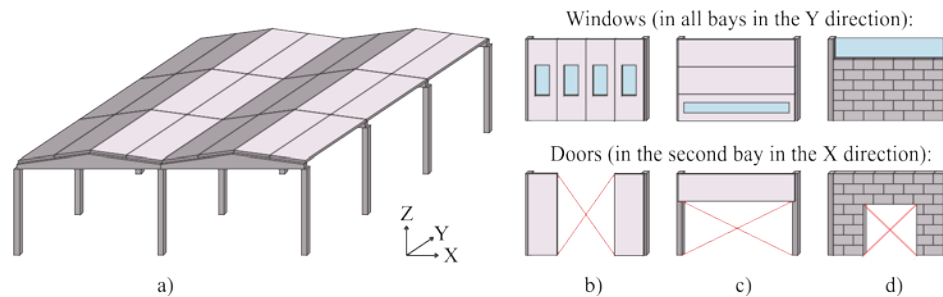


Fig. 2 – a) Structural configuration of investigated buildings, b) location of windows and doors in vertical panels, c) location of windows and doors in horizontal panels, and d) location of windows and doors in masonry infills.

The vertical and horizontal precast panels are attached to the beams and columns, respectively [13]. At the bottom, the vertical panels are restrained by a foundation beam, whereas the horizontal panels are placed on vertical supports, which are fixed to the columns [13]. The corbels prevent vertical and out-of-plane horizontal displacements, but permit a certain level of in-plane horizontal drift due to a gap, which is provided for the installation of the panels. At the top of both the vertical and the horizontal panels, fastenings are provided. In the case of the vertical panels, fastening A is used, consisting of a hammer-head strap, which connects the steel channels, which are embedded in the panel, to the supporting structural element. In the case of the horizontal panels, fastenings B and C are used in addition to the fastening A. They contain a steel angle element and a steel box element, respectively. In one direction (frames in the X direction) doors were considered by taking out two panels in the second bay (Figs. 2b and 2c). In the other direction (frames in the Y direction) windows were considered by reducing the mass of the panels. In the case of horizontal panels, only the bottom panel was considered to have windows. Furthermore, masonry infills are situated between the columns and have poor connections with the adjacent beams. No out-of-plane restraints are provided. In one direction (the frames in the X direction) doors of a constant height and a varying length were considered. In the other direction (frames in the Y direction) windows reaching from column to column were considered in each bay (Fig. 2d). In Table 4 distributions of the non-structural components' random parameters are presented.



Table 2 – Geometric parameters of buildings. θ and β represent the median and the standard deviation in the log domain, respectively, describing the beam length (L_{beam}), the distance between portals (L_{intercol}), and the column height (H_{col}). The length (L_{corbel}) and height (h_{corbel}) of the corbels are given as a function of the beam length [10].

Parameter		
L_{beam} [m]	Lognormal distribution ($\theta = 14.9; \beta = 0.3$)	
L_{intercol} [m]	Lognormal distribution ($\theta = 6.8; \beta = 0.28$)	
H_{col} [m]	Lognormal distribution ($\theta = 6.5; \beta = 0.25$)	
L_{corbel} [m]	$L_{\text{beam}} < 18$ m	0.25
	$18 \text{ m} < L_{\text{beam}} < 25$ m	0.35
	$L_{\text{beam}} > 25$ m	0.45
h_{corbel} [m]	$L_{\text{beam}} < 18$ m	0.35
	$18 \text{ m} < L_{\text{beam}} < 25$ m	0.45
	$L_{\text{beam}} > 25$ m	0.55

Table 3 – Uniformly distributed values of characteristic concrete compressive strength (R_{ck}) and characteristic yield strength of the reinforcement (f_{sk}) used in the design of buildings [10].

Parameter	
R_{ck} [MPa]	35, 40, 45, 50
f_{sk} [MPa]	320 (smooth), 380 (ribbed)

Table 4 – Minimum and maximum values of the uniformly distributed parameters of the non-structural components – combined thickness of the concrete layers in the vertical and horizontal panels (t_{panel}), the fraction of glazed area in the vertical panels in the Y direction ($A_{\text{glazed,vertical}}$), the fraction of glazed area in the bottom horizontal panel in the Y direction ($A_{\text{glazed,horizontal}}$), the thickness of the masonry infills (t_{infill}), the volumetric weight of the masonry infills (γ_{infill}), window height in the buildings with masonry infills (h_{window}), and door length in the buildings with masonry infills (L_{door}) [12].

Parameter	Min	Max	Reference
t_{panel} [cm]	16	18	[13]
$A_{\text{glazed,vertical}}$ [%]	7.5	20	[14], Field inspections ¹
$A_{\text{glazed,horizontal}}$ [%]	50	90	[14], Field inspections ¹
t_{infill} [cm]	20	30	[15]
γ_{infill} [kN/m ³]	13.6	14.4	[16, 17]
h_{window} [m]	1	2	Field inspections ¹
L_{door} [m]	2	4	Field inspections ¹

3. Numerical models of precast buildings for non-linear dynamic analysis

A lumped plasticity model, as presented in [12], was developed for each building using OpenSees software [18]. The principles which were applied when modelling the load-bearing structures (Fig. 3) were the same in the case of all of the investigated building classes. In the case of building classes which included non-structural components (Table 1) additional elements were added to the model of load-bearing structure. A summary of the

¹ Data obtained on the basis of field inspections by the authors of the paper.

description of models is provided in Sections 3.1, 3.2 and 3.3. For more details on the numerical models a reader is referred to [12].

The seismic response of the investigated buildings was simulated by nonlinear dynamic analysis taking into account the X, Y and Z components of the ground motions. The coefficients of the model of Rayleigh damping were estimated from the vibration periods, which corresponded to the secant stiffness associated with yielding of the columns, by assuming a 2% damping ratio. The P- Δ effect was also taken into account.

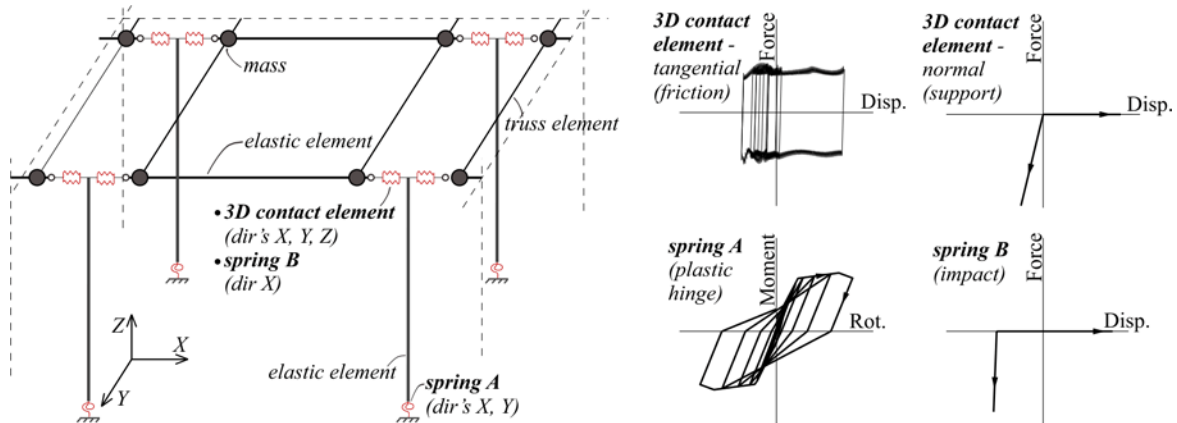


Fig. 3 – Schematic illustration of a section of a model of the load-bearing structure with the force-displacement (moment-rotation) relationship of the non-linear elements used in the model.

3.1 Load-bearing structures

The columns were modelled by one component lumped plasticity elements with two independent rotational springs (about the X and Y directions) which were located at the base of the columns (spring A, Fig. 3). Each spring was defined by a four-linear moment-rotation relationship according to previous studies [12, 19]. Elastic elements were used for the beams with concentrated masses at their endpoints. The frictional connections between the beams and columns were modelled by a 3D contact zero-length element. The friction coefficient was determined according to [20], whereas no cohesion was assigned. The effect of beam-to-column impact was simulated by an elastic no-tension spring with an initial gap (spring B in Fig. 3), which was modelled in parallel with the 3D contact zero-length element. The effect of the lateral beams and roof elements was modelled by truss elements, which were assumed to be elastic and pinned to the beam.

3.2 Vertical and horizontal panels

The effect of vertical panels was modelled by simulating only the response of the fastenings (Fig. 4, top left). In this case, only fastenings A were considered. Fastenings of one half of the panels in a bay were modelled by two independent springs (C and D, Fig. 4), connecting beams to nodes, which were fixed in the in-plane (i.e. parallel to the plane of the panels) direction. The first spring was modelled in the in-plane direction and was defined on the basis of cyclic tests [21] by three springs in parallel, i.e. an elastic perfectly plastic spring, and two elasto-plastic springs with an initial gap [12, 22]. The second spring was modelled in the out-of-plane (i.e. perpendicular to the plane of the panels) direction and was considered elastic. Moreover, in the out-of-plane direction, one half of the mass of the panels was assigned, the other one being transferred directly to the ground.

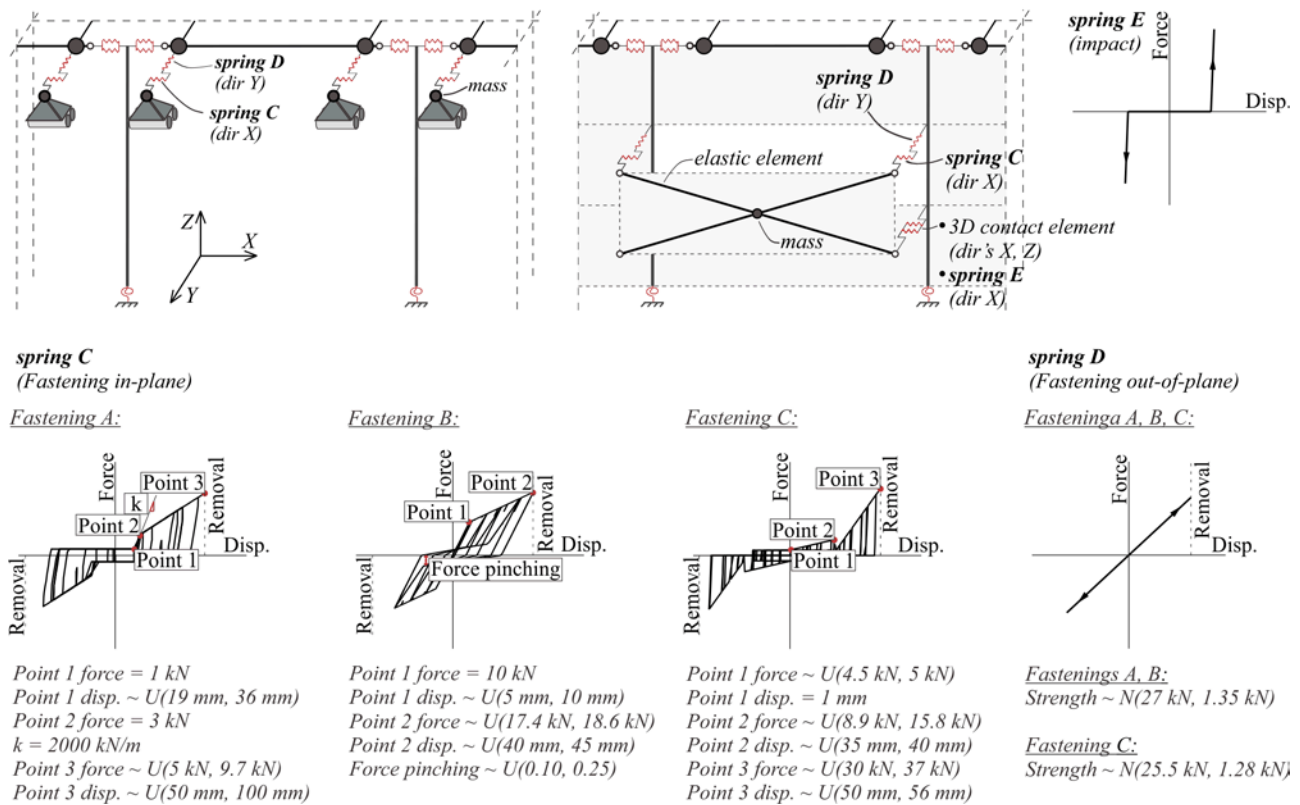


Fig. 4 – Schematic illustrations of sections of models of the building with vertical panels (top left) and the building with horizontal panels (top right) with the force-displacement relationship of the non-linear elements used in the models. Some parameters of the non-linear elements are considered constant, whereas others are uniformly or normally distributed.

The horizontal panels were modelled by elastic elements with high stiffness, which were attached to the columns (Fig. 4, top right). A mass was assigned to the centre of each panel. The connections at the bottom of the panels were modelled by two elements connected in parallel, i.e. by a 3D contact zero-length element, which was used to simulate the vertical support and the friction, and a multilinear spring whose purpose was to simulate the impact of the panel in the in-plane direction (spring E, Fig. 4). At the top of each panel, the fastenings were modelled by two independent springs. All three types of fastenings were considered in this case. In the in-plane direction, fastenings A were modelled in the same way as in the case of the vertical panels, whereas fastenings B and C were modelled, respectively, by a bilinear hysteretic spring, and by five springs in parallel – an elastic, perfectly plastic spring, and four elasto-plastic springs with an initial gap (spring C, Fig. 4). In the out-of-plane direction fastenings were modelled by an elastic spring (spring D, Fig. 4).

In the case of both the vertical and the horizontal panels, the criteria for the in-plane and out-of-plane failure of the fastenings were controlled by defining the ultimate displacements (Fig. 4). If any of the criteria for a given fastening were met, the panel, which was connected to the structure by that particular fastening, was considered to be dislocated and was removed from the model during further analysis.

3.3 Masonry infills

Masonry infills were modelled by stiff elastic elements and rigid constraints with their mass concentrated at the centre of the infill (Fig. 5). At the bottom, infills were connected to the fixed nodes by two elastic-no tension springs, in order to enable rocking of the infills in the out-of-plane direction (spring F, Fig. 5). At the top, infills were connected to the columns by a 3D impact zero-length element, which enabled the development of frictional forces in the out-of-plane direction and impact in the in-plane direction of the infills. The former was modelled

as in the case of the 3D contact zero-length elements, whereas the latter was defined by a bi-linear force-displacement relationship [23, 24]. Openings were accounted for by reducing the stiffness and strength of the infills as suggested in [25]. If either the in-plane strength or the out-of-plane critical rotation (associated with the infill's centre of gravity being just above its hinge) was reached, the infill was considered dislocated, and was immediately removed from the model during the analysis. Note that the model of any column was also upgraded by an additional rotational spring (spring A), if the adjacent masonry infill was not constructed to the top of the column due to windows. In this case an additional plastic hinge was inserted in the column at the point of its contact with the top of the infill in order to capture the non-linear behaviour of the column.

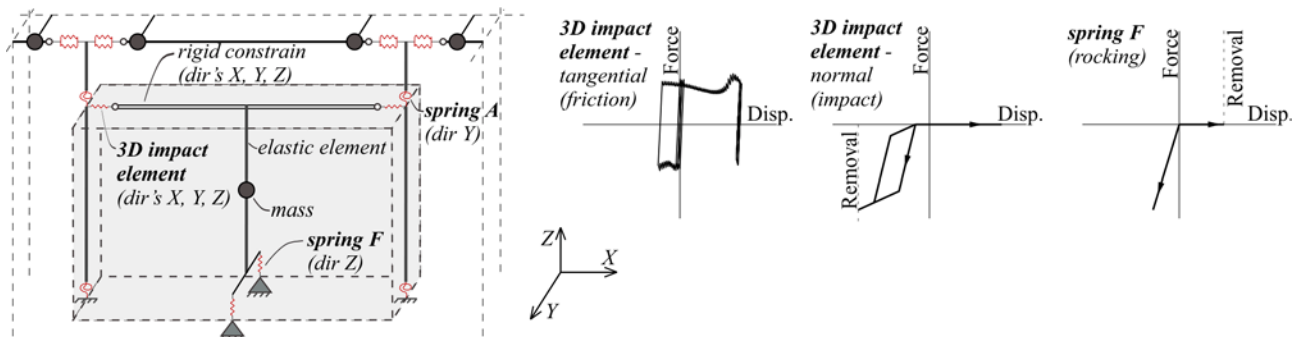


Fig. 5 – Schematic illustrations of a section of a model of the building with masonry infills with the force-displacement relationship of the non-linear elements used in the model.

4. Methodology for fragility analysis of the investigated building classes

In this study the methodology which was originally proposed in [10] and modified in [12] is used. Each building class was represented by a sample of 100 buildings. The load-bearing structures were determined through simulated design [10] in order to take into account the variations in the geometry and mechanical properties. Monte Carlo simulation was used to generate the sample values. This method was also used for the generation of the sample of the non-structural components and uncertain modelling parameters. For every building a numerical model was then defined. The seismic performance of each building from a sample of 100 buildings was investigated for 70 seismic events. These events were considered to be equal to those used in [10]. All nonlinear dynamic analyses were performed with the OpenSees software [18].

In each simulation, two types of damage states, i.e. a non-structural and a structural damage state were determined. Non-structural damage was defined by one of the four damage states, which corresponded to different portions of the dislocated non-structural components, i.e. no component dislocated (DS-0), at least one component dislocated (DS-1), at least one half of components dislocated (DS-2) and all the components dislocated (DS-3). The criteria for the dislocation of non-structural components are described in Section 3. Furthermore, structural damage was defined by one of the three damage states, i.e. no or slight damage (DS-NS), moderate damage (DS-M) or structural collapse (DS-C). Moderate damage was defined as a sequence of either of the following:

- Rotation in at least one column exceeded the yield rotation, which was determined according to a previous study [19].
- Displacement in at least one beam-to-column connection exceeded the value which indicated the initiation of sliding (1 cm).

Structural collapse was defined as a sequence of either:

- The collapse of at least one column, which was defined when the rotation in the plastic hinge of the column exceeded the ultimate rotation [26], which corresponded to 80% of the column's strength, if measured in the post-capping range.
- The unseating of a beam in at least one beam-to-column connection, which occurred if the relative beam drift exceeded the sliding capacity, which was assumed to be equal to the length from the edge of the beam to the edge of the corbel.



Dependency between the non-structural and the structural damage was accounted for by considering all the non-structural components to be dislocated in the case of structural collapse.

For a given seismic event and a given damage state, a ratio between the number of the sample buildings meeting the designated damage state and the total number of simulated buildings was calculated. Once the seismic events were quantified by a certain level of the selected intensity measure, a regression analysis was performed, which provided the moments of the collapse fragility functions, i.e. the median seismic intensities causing designated limit states and the corresponding standard deviations in the log domain. The geometric mean of the peak ground accelerations in both horizontal components was used for the intensity measure, since it is an intensity measure which is independent of the building class concerned. The regression analysis was carried out by assuming a lognormal distribution and by using the maximum likelihood method as proposed in previous studies [27, 28]. An example of simulation data and the corresponding fragility curves for two damage states are shown in Fig. 6a, whereas an illustration of determining different damage states probability based on fragility curves is given in Fig. 6b.

5. Results and discussion

In this section, parameters of fragility curves for non-structural damage are first presented. This is followed by the presentation of the fragility curves for structural damage and the inspection of the impact that non-structural components have on them. Finally, the effect of non-structural components is illustrated by an example of a non-linear dynamic analysis.

It was observed that fragility curves for non-structural damage states depend substantially on the type of non-structural components (Table 5). This is most significant in the case of DS-1 (first component dislocated), where the values of \tilde{a}_g for buildings with masonry infills and buildings with vertical panels, respectively, exceed \tilde{a}_g associated with buildings with horizontal panels for approximately 50 % and 200 %. However, the difference in performance is less when inspecting fragility curves for DS-2 (at least one half of non-structural components dislocated) and DS-3 (all non-structural components dislocated). Moreover, it was observed that the type of fastenings had little impact on the fragility curves of buildings with horizontal panels. Nevertheless, the best performance was observed in the case of fastenings A, whereas panels attached with fastenings C were dislocated at the lowest levels of intensity.

Table 5 – Fragility parameters (median and logarithmic standard deviation) for all the considered classes of buildings

Building Class	DS-1		DS-2		DS-3		DS-M		DS-C	
	\tilde{a}_g [g]	$\sigma_{\ln a_g}$								
1	/	/	/	/	/	/	0.11	0.46	0.60	0.22
2	0.42	0.38	0.52	0.29	0.55	0.26	0.11	0.48	0.56	0.25
3	0.13	0.46	0.29	0.48	0.46	0.43	0.10	0.32	0.48	0.43
4	0.13	0.44	0.26	0.46	0.42	0.45	0.10	0.30	0.44	0.45
5	0.12	0.46	0.25	0.49	0.41	0.47	0.10	0.33	0.43	0.47
6	0.19	0.72	0.30	0.61	0.46	0.39	0.09	0.21	0.59	0.26

Structural damage states were influenced by the type of non-structural components as well (Table 5, Fig. 6c). While vertical panels had no significant impact on moderate damage, the addition of horizontal panels and masonry infills reduced both \tilde{a}_g and $\sigma_{\ln a_g}$. In the case of horizontal panels, the reductions amounted to approximately 10 % and 30 %, respectively, whereas masonry infills reduced the fragility parameters for about 20 % and 50 %, respectively. Furthermore, non-structural components also affected structural collapse. In the cases of buildings with vertical panels and masonry infills, a small reduction in \tilde{a}_g was observed, whereas $\sigma_{\ln a_g}$ was slightly increased. Both of these changes in parameters, according to [29], lead to a higher probability of



collapse. The impact of horizontal panels was even more significant. Their inclusion in the structure decreased \tilde{a}_g for approximately 25 % and increased $\sigma_{\ln a_g}$ for about 100 %.

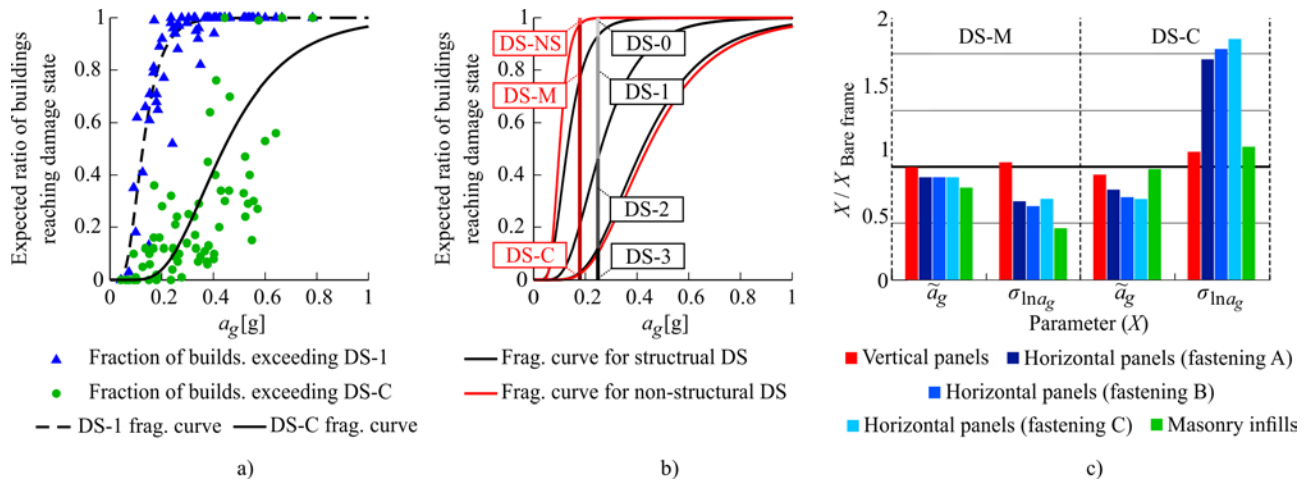


Fig. 6 – a) Fractions of buildings within building class 4 exceeding DS-1 and DS-C with the corresponding fragility curves, b) fragility curves of building class 2 with highlighted probabilities of occurrence of non-structural and structural damage states given the two level of peak ground acceleration, and c) parameters of fragility curves (median and logarithmic standard deviation) of classes of buildings with non-structural components normalized to parameters of building class 1 (bare frame buildings) fragility curve.

Several phenomena contribute to such differences in fragility curves. Some of them are illustrated in Fig. 7a, where time-histories for rotation in the plastic hinges of columns and displacements at the corresponding beam-to-column connections are presented for four buildings with the same structure but different type of non-structural components. Only one building with horizontal panels (the one with fastenings B) is represented, since all of them exhibit similar results. The time-history records of rotations around the X axis (due to the drifts in the direction of the Y axis) and displacements in the direction of the Y axis are presented for plastic hinges at the bases of three columns and for three beam-to-column connections, respectively. The following observations can be made. Firstly, the largest rotations were recorded in buildings with horizontal panels (Columns B, C). This is contributed by the mass of the panels causing inertial forces which act below the beam-to-column connection and prevail over the effect of the increased stiffness in the plane of Column C. However, rotations in the internal column (Column A) are similar to those recorded in other types of buildings. This is because frictional beam-to-column connections are not able to transfer all of the inertial forces, which are caused by the horizontal panels. For the same reason, displacements in the beam-to-column connections in this particular building are larger than those in the connections of the bare frame building (Connections 1, 2, 3). Secondly, masonry infills increase stiffness in the in-plane direction (parallel to their own plane) and thus reduce the rotations at the bases of the columns (Column C). However, this increases the demand in the beam-to-column connections, which leads to larger displacements in comparison with the bare frame building (Connection 3). Thirdly, inertial forces due to mass of vertical panels cause larger displacements in Connections 1 and 2. On the contrary, displacements in Connection 3 are smaller than those in the bare frame building. Such an observation may be contributed to the increase in stiffness due to the panels along the Y axis. In this case the increase in stiffness is beneficial (conversely to the case of building with masonry infills), since the panels are attached to the structure above the beam-to-column connection, which means that a certain amount of forces is transferred through the panels to the ground. The example presented herein was chosen, since it corresponds to a small fraction of dislocated non-structural components. In cases where more components were dislocated, their effect might not be as significant. Moreover, the phenomena presented above should be understood qualitatively, i.e. it was observed that the severity of the impact of a certain phenomenon differs case by case.

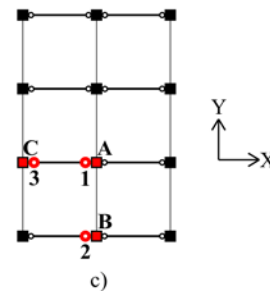
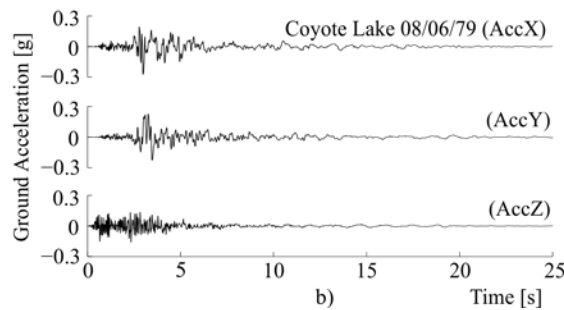
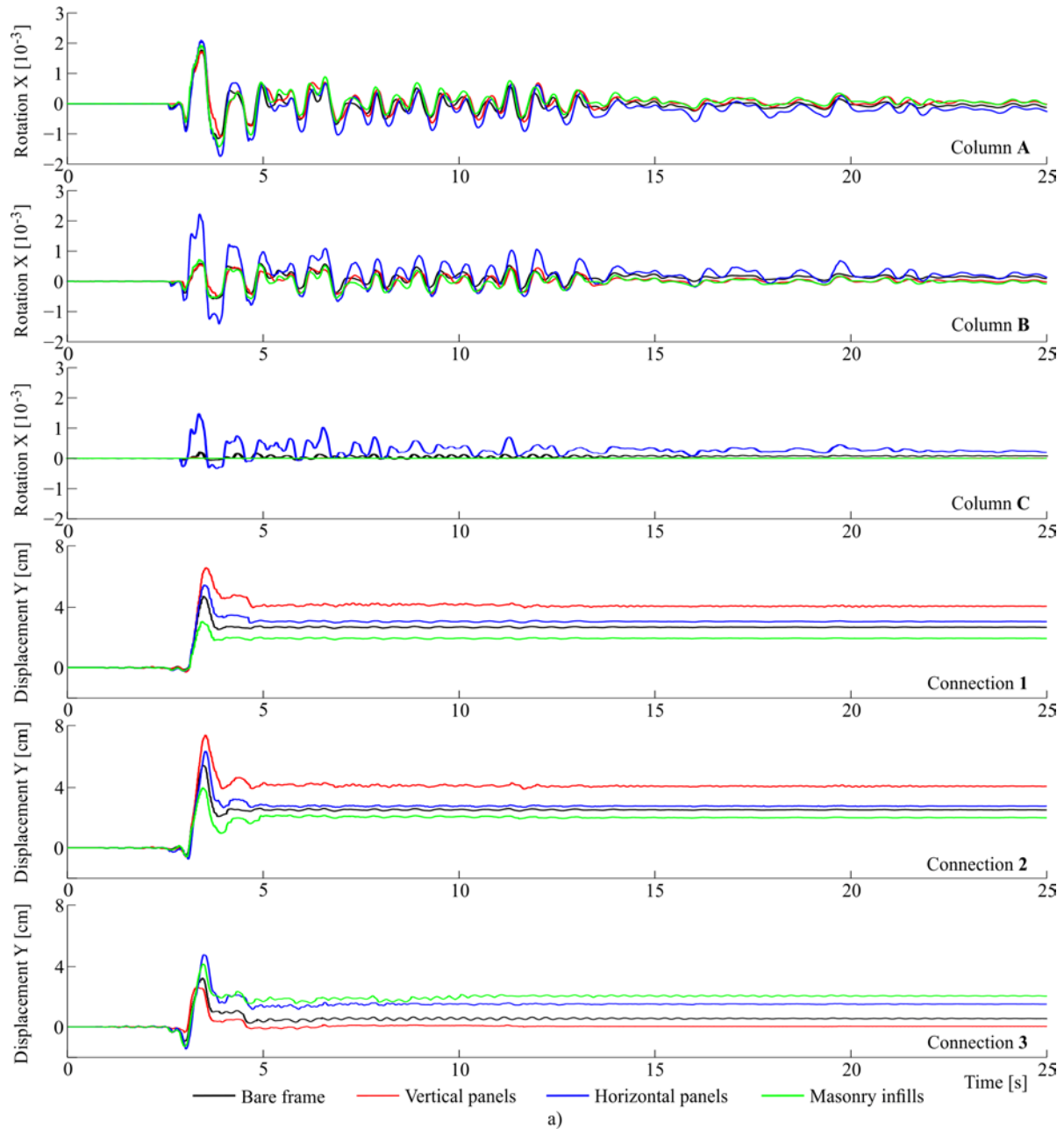


Fig. 7 – a) Results of non-linear dynamic analyses of four buildings with the same structure (bare frame) but different non-structural components (vertical panels, horizontal panels and masonry infills), b) ground acceleration of the seismic event used in analyses and c) plan view of the structure with highlighted locations of columns A-C and connections 1-3.



6. Conclusions

Fragility curves for six classes of precast RC buildings with the same structure but different type of non-structural components were presented. Four damage states corresponding to non-structural damage and three damage states corresponding to structural damage were considered.

It was observed that both structural and non-structural damage depend on the type of the non-structural components. For both types of damage, buildings with horizontal panels exhibited the worst performance, followed by buildings with masonry infills and buildings with vertical panels. By adding horizontal panels to the bare frame structure, the median peak ground acceleration causing collapse decreased for about 25 %, whereas the logarithmic standard deviation increased for about 100 %.

Phenomena which contribute to these differences in fragility curves were illustrated by time-histories of selected analyses which were used in the fragility analysis. It was shown that the inertial forces perpendicular and parallel to the plane of the horizontal panels increased displacements in beam-to-column connections as well as rotations in columns despite the increased stiffness of the structure caused by the horizontal panels oriented in the parallel direction. If masonry infills were used in the investigated precast buildings, stiffness of the structure was reduced, which caused smaller rotations in columns but larger displacements in beam-to-column connections. In the case of buildings with vertical panels, displacement demand in beam-to-column connections, measured perpendicular to the plane of the panels, was significantly increased because of large additional inertial forces and negligible effect on stiffness. However, the effect of increased stiffness in the direction parallel to the plane of the panels was found beneficial in this case, since the vertical panels were attached to the roof which helped to reduce the demand in the beam-to-column connections. It can therefore be concluded that mass of non-structural components generally has a detrimental effect on the performance of precast buildings, whereas the effect of increased stiffness is more unfavourable if non-structural components are attached to the structure below the beam-to-column connection rather than above it. Furthermore, the severity of their impact varies due to the dispersion of their strength, which affects the time of their potential dislocation. This increases the dispersion of levels of intensity causing designated damage states reflected in fragility curves.

7. Acknowledgements

The results presented in this paper are based on work which was supported by the 7th EU framework research project STREST “Harmonized approach to stress tests for critical infrastructure against natural hazards” and by the Slovenian Research Agency.

8. References

- [1] Toniolo G, Colombo A (2012): Precast concrete structures: the lessons learned from the L’Aquila earthquake. *Structural Concrete*, **13** (2), 73-83.
- [2] Magliulo G, Ercolino M, Petrone C, Coppola O, Manfredi G (2014): The Emilia earthquake: Seismic performance of precast reinforced concrete buildings. *Earthquake Spectra*, **30** (2), 891-912.
- [3] Bournas DA, Negro P, Taucer FF (2013): Performance of industrial buildings during the Emilia earthquakes in Northern Italy and recommendations for their strengthening. *Bulletin of Earthquake Engineering*, **12** (5), 2383-404.
- [4] Belleri A, Brunesi E, Nascimbene R, Pagani M, Riva P (2015): Seismic performance of precast industrial facilities following major earthquakes in the Italian territory. *Journal of Performance of Constructed Facilities*, **29** (5), 04014135.
- [5] Casotto C (2013): Seismic vulnerability of Italian RC precast industrial structures. *Masters dissertation*, Università degli Studi di Pavia, Istituto Universitario di Studi Superiori di Pavia, Pavia, Italy.
- [6] Colombo A, Negro P, Toniolo G (2014): The influence of claddings on the seismic response of precast structures: The Safelcladding project. *Second European conference on earthquake engineering and seismology*, Istanbul, Turkey.
- [7] Ercolino M, Magliulo G, Coppola O, Manfredi G (2014): Code formula for the fundamental period of RC precast buildings. *Second European conference on earthquake engineering and seismology*, Istanbul, Turkey.



- [8] Belleri A, Torquati M, Riva P, Nascimbene R (2015): Vulnerability assessment and retrofit solutions of precast industrial structures. *Earthquakes and Structures*, **8** (3), 801-20.
- [9] Senel SM, Kayhan AH (2010): Fragility based damage assesment in existing precast industrial buildings: A case study for Turkey. *Structural Engineering and Mechanics*, **34** (1), 39-60.
- [10] Casotto C, Silva V, Crowley H, Nascimbene R, Pinho R (2015): Seismic fragility of Italian RC precast industrial structures. *Engineering Structures*, **94**, 122-36.
- [11] Korkmaz KA, Karahan AE (2011): Investigation of seismic behavior and infill wall effects for prefabricated industrial buildings in Turkey. *Journal of Performance of Constructed Facilities*, **25** (3), 158-71.
- [12] Babič A, Dolšek M (2016): Seismic fragility functions of industrial precast building classes. *Engineering Structures*, **118**, 357-70.
- [13] Isaković T, Fischinger M, Karadogan F, Kremmyda GD, Dal Lago B, Pegan A, et al. (2012): Improved fastening systems of cladding wall panels of precast buildings in seismic zones. *SAFECLADDING, Deliverable 1.1*, University of Ljubljana, Ljubljana, Slovenia.
- [14] Tre Colli: Schede Tecniche, Elementi prefabbricati. http://www.impresatrecolli.com/img/design_specifications.pdf (accessed January 4, 2016).
- [15] Magrini A, Martino A, Murano G (2011): Trasmittanza termica. Comitato Termotecnico Italiano Energia e Ambiente, Milano, Italy.
- [16] MIT (2009): Circolare 2 febbraio 2009, n. 617 Istruzioni per l'applicazione delle «Nuove norme tecniche per le costruzioni» di cui al decreto ministeriale 14 gennaio 2008. Rome, Italy.
- [17] F.lli Vacis Group: Blocchi splittati e scanalati. http://www.vacissrl.it/allegati/download/catalogo_blocchi_per_sito_senza_nr_pagina_136627419554984.pdf (accessed January 5, 2016).
- [18] McKenna F, Fenves GL (2010): Open System for Earthquake Engineering Simulation (OpenSees). Pacific Earthquake Engineering Research Center, Berkeley, USA. <http://opensees.berkeley.edu>.
- [19] Dolsek M (2010): Development of computing environment for the seismic performance assessment of reinforced concrete frames by using simplified nonlinear models. *Bulletin of Earthquake Engineering*, **8** (6), 1309-29.
- [20] Magliulo G, Capozzi V, Fabbrocino G, Manfredi G (2011): Neoprene-concrete friction relationships for seismic assessment of existing precast buildings. *Engineering Structures*, **33** (2), 532-8.
- [21] Isaković T, Zoubek B, Lopatič J, Urbas M, Fischinger M (2013): Report and card files on the tests performed on existing connections. *SAFECLADDING, Deliverable 1.2*, University of Ljubljana, Ljubljana, Slovenia.
- [22] Babič A, Dolšek M (2014): The impact of structural components on fragility curves of single-storey industrial precast structures. *Second European conference on earthquake engineering and seismology*, Istanbul, Turkey.
- [23] Panagiotakos TB, Fardis MN (1996): Seismic response of infilled RC frame structures. *The Eleventh world conference on earthquake engineering*, Acapulco, Mexico.
- [24] Fardis MN (1996): Experimental and numerical investigations on the seismic response of RC infilled frames and recommendations for code provisions. Laboratorio Nacional de Engenharia Civil, Lisbon, Portugal.
- [25] Dawe JL, Seah CK (1988): Lateral load resistance of masonry panels in flexible steel frames. *The Eighth International Brick and Block Masonry Conference*, Dublin, Republic of Ireland.
- [26] CEN (2005): Eurocode 8: Design of structures for earthquake resistance - Part 3: Assessment and retrofitting of buildings. European Committee for Standardisation, Brussels, Belgium.
- [27] Baker JW (2015): Efficient analytical fragility function fitting using dynamic structural analysis. *Earthquake Spectra*, **31** (1), 579-99.
- [28] Baker JW (2015): Code supplement to efficient analytical fragility function fitting using dynamic structural analysis. <http://purl.stanford.edu/sw589ts9300> (accessed January 5, 2016).
- [29] Cornell CA (1996): Calculating building seismic performance reliability: A basis for multi-level design norms. *The Eleventh world conference on earthquake engineering*, Acapulco, Mexico.